International Journal of Environmental Sciences
ISSN: 2229-7359
Vol. 11 No. 23s, 2025
https://theaspd.com/index.php

Synthesis and Evaluation of Novel Quinazolinone-Conjugated Triazole Hybrids as Anti-Glycation Agents: An Integrated Experimental and in Silico Approach

Ashutosh Patankar[1], Achal Mishra[2], Mukesh Sharma[3], Dhansay Dewangan[4]
[1]Research Scholar, Shri Shankaracharya Technical Campus (SSTC) - Shri Shankaracharya Group of Institutions (SSGI) - Faculty of Pharmaceutical Sciences (FPS), Bhilai, CG. India
[2]Department of Pharmacy, Guru Ghasidas Vishwavidyalaya,Bilaspur, CG, India
[3]Rungta College of Pharmaceutical Sciences and Research, Bhilai,CG, India
[4]Department of Chemistry, Govt. Lahiri PG College, Chirmiri,CG, India
Corresponding Author: Dr. Dhansay Dewangan,Email: dhansaydewangan@gmail.com

Abstract
*In the present study, a series of Quinazolinone-triazole hybrids (**2a-j**) were developed and assessed as multi-therapeutic compounds against hyperglycemia and glycation-induced diabetic complications. These agents are designed to competitively halt the bonds between monosaccharides and serum proteins in the glycation process. Structural elucidation was carried out by various spectroscopic techniques, and their biological activities were evaluated in vitro through UV-visible spectroscopy-based assays. The most active α-glycosidase inhibitory activity of compounds **2d** and **2h,** with IC_{50} values 58.33±0.88 µM and 46.00±1.15 µM, respectively, was found among these synthesized hybrids with improved activity compared to the standard rutin (IC_{50}= 75.33±1.45 µM). These potent compounds also blocked the production of advanced glycation end products (ACEs) as evidenced by their fructosamine level estimation (IC_{50}: 2d = 66.66±0.88µM, and 2h = 53.33±1.76 µM). Further, these derivatives represented the strong antioxidant potential (IC_{50}: 2d=25.66±0.88 µM and 2h=34.00±1.00 µM) over ascorbic acid. The result of biological activity suggested that the electron-donating groups, especially the alkyl group, exhibited strong activity over the electron-withdrawing group. The simulation results of molecular docking supported that the stronger molecular interaction could be attributed to the introduction of the electron-donating groups that led to a higher bioactivity of these derivatives. Overall, the findings suggest that Quinazolinone-triazole hybrids are potentially useful multi-therapeutic agents in the treatment of diabetic conditions and the glycation process-related complications.*
Keywords: *Quinazolinone-triazole hybrid, Antiglycation activity, α-glycosidase inhibitory activity, antioxidant activity, multi-therapeutic agent, Diabetic condition.*

1. INTRODUCTION

Advanced glycation end products (AGEs) are formed through a non-enzymatic reaction known as the Maillard reaction, in which reducing sugars react with free amino groups of proteins, lipids, or nucleic acid [1]. This multi-step reaction initially involves the formation of reversible Schiff bases, which subsequently rearrange into more stable Amadori products. Further, these intermediates undergo oxidative modifications and molecular cross-linking, ultimately leading to the formation of stable advanced glycation end products (AGEs) [2-3]. The production and accumulation of AGEs are significantly enhanced under hyperglycemic conditions. The accumulation of AGEs in the tissues plays a crucial role in the development and progression of various chronic disorders [4]. AGEs may modify structural and functional characteristics of biomolecules, affect cell signaling, and trigger oxidative stress and inflammation by binding to particular receptors, notably the AGE receptor (RAGE) [5]. The processes are involved in the development of diabetic complications including nephropathy, retinopathy, neuropathy, and cardiovascular diseases (Figure 1) [6].Therefore, inhibiting AGEs formation has emerged as a promising strategy for preventing or delaying glycation-associated disorders.

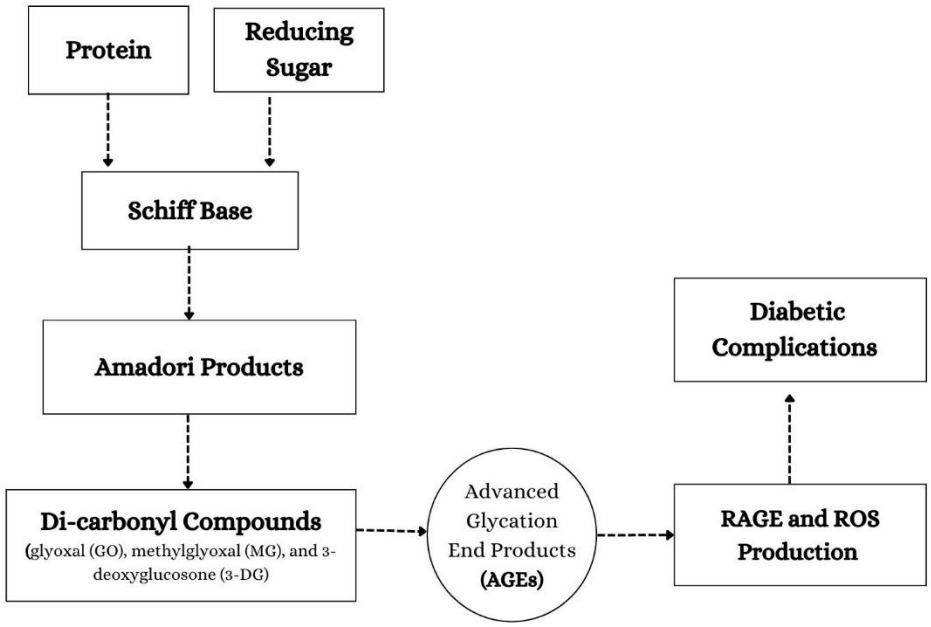

Among various chemical scaffolds, quinazolinone and 1,2,4-triazoles have emerged as versatile heterocycles with significant antioxidant and antidiabetic properties [7]. Their structural features, such as the ability to participate in hydrogen bonding and π–π stacking, make them attractive candidates for antiglycation drug development [8]. Combining these moieties is expected to enhance bioactivity through synergistic interactions at glycation-prone protein sites. Despite the therapeutic potential of both quinazolinone and triazole systems, there is a noticeable research gap concerning their hybrid structures as antiglycation agents. Limited studies have focused on the molecular design, synthesis, and biological evaluation of quinazolinone triazole hybrids specifically targeting AGE formation. Additionally, there is a lack of detailed molecular docking studies to explain the mechanism of antiglycation action at the protein level, especially with key residues in human serum albumin (HSA) [9].

Although quinazolinone triazole scaffolds are known for their diverse pharmacological activities, their hybrid structures remain largely unexplored as antiglycation agents. Existing studies rarely investigate the combined efficacy of these agents or provide comprehensive details about their interactions with glycation-prone proteins, such as human serum albumin (HSA). The lack of integrated in vitro and in silico evaluations underscores the need for systematic research on quinazolinone triazole derivatives to assess their potential as effective antiglycation therapeutics. The prospects of quinazolinone triazole-based derivatives are promising, with the potential to serve as lead candidates for the treatment of glycation-related disorders such as diabetes and its complications.

2. MATERIALS AND METHODS

2.1Chemicals

All chemicals and solvents used in the synthesis were of analytical grade and sourced from Sigma Aldrich, Merck, SRL Chemicals, Loba Chemie, and CDH Chemicals. The study utilized bovine serum albumin (BSA), α-glycosidase enzyme (Saccharomyces cerevisiae), Rutin, p-nitrophenyl-α-D-glucopyranoside (pNPG), fructose, nitro blue tetrazolium (NBT), dimethyl sulphoxide (DMSO), 5,5'-dithiobis (2-nitrobenzoic acid) (DTNB), 2,4-dinitrophenylhydrazine (DNPH), and Congo red, 2,2-diphenyl-1-picrylhydrazyl (DPPH). The thin layer chromatography on silica gel G plate (E. Merck) was utilized to observe the reaction's progress and completion. Structural characterization was performed using ^{1}H NMR and ^{13}C NMR spectroscopy on a Bruker Advance Neo 400 MHz spectrometer with DMSO-D_6 as the solvent. Infrared (IR) spectra were recorded on a PerkinElmer Spectrum IR version 10.6.2 FTIR spectrophotometer, while mass spectra were acquired on an Xevo G2-XS QT quadrupole time-of-flight (QTOF) mass spectrometer. The Thermo Scientific Flash 2000 analyzer was employed for elemental analysis

2.2Synthesis

2.2.1 General Procedure for Synthesis of (2-phenyl-4H-3,1-benzoxazin-4-one **(1a-j)**[10]

Anthranillic acid (0.01mol) was dissolved in pyridine (50 mL) by maintaining the temperature at 8℃. An equivalent amount of substituted benzoyl chloride was added dropwise with stirring over 1 hour, and the stirring was continued for an additional 2 hours at room temperature. The resulting precipitate was collected by filtration after neutralization with aqueous $NaHCO_3$, washed with water, and recrystallized from ethanol to afford pale yellow crystals.

2.2.2 General procedure for the synthesis of compound **(2a-j)**

The stoichiometric mixture of compound (1a-j) (0.01 mol) and 4-amino triazole was dissolved in dry pyridine (60 mL) and refluxed for 5 hours at 90-100℃. The reaction mixtures were cooled and poured into ice-cold water; the precipitate obtained was filtered, dried, and crystallized with ethanol.

2-phenyl-3-(1H-1,2,4-triazol-3-yl)quinazolin-4(3H)-one (2a)

Color: canary yellow powder; m.p. 186-188°C; % yield: 66-68%; IR (KBr, cm^{-1}): 3064.40 (Ar C-H), 1667.02 (C=O), 1578.98 (C=C), 1526.29 (C=N), 1344.96 (C-N), 838.30 (N-N);^{1}HNMR (400 MHz, DMSO-d_6): δ 7.49-7.68 (5H, m, ArCH), 7.76-8.12 (4H, m, ArCH), 7.63 (1H, d, C-$H_{triazole}$), 14.46 (1H, s, $NH_{triazole}$); ^{13}CNMR (125 MHz, DMSO-d_6), δppm: 120.7 (1C), 126.5-126.7 (2C), 127.3 (1C), 128.2-128.8 (5C), 130.1 (1C), 133.4 (1C), 146.1 (1C), 148.0-148.7 (2C), 156.2 (1C), 160.5 (1C, >C=O); MS m/z: 289.26 [M^+] calculated for $C_{16}H_{11}N_5O$; Elemental Analysis calculated: C, 66.43; H, 3.83; N, 24.21; O, 5.53; Found: C, 66.57; H, 3.94; N, 24.28; O, 5.61.

2-(4-chlorophenyl)-3-(1H-1,2,4-triazol-3-yl)quinazolin-4(3H)-one (2b)

Color: light yellow powder; m.p. 157-159°C; % yield: 62-65%; IR (KBr, cm^{-1}): 3085.01 (Ar C-H), 1667.57 (C=O), 1578.88 (C=C), 1527.02 (C=N), 1345.14 (C-N), 839.06 (N-N);^{1}HNMR (400 MHz, DMSO-d_6): δ 7.39-7.49 (4H, m, ArCH), 7.50 (1H, d, ArCH), 7.68 (1H, s, ArCH), 7.85 (1H, d, ArCH), 8.12 (1H, s, ArCH), 7.62 (1H, d, C-$H_{triazole}$), 14.46 (1H, s, $NH_{triazole}$); ^{13}CNMR (125 MHz, DMSO-d_6), δppm: 120.8 (1C), 126.6-126.7 (3C), 127.3 (1C), 128.9-129.1 (4C), 133.3 (1C), 135.6 (1C), 146.1 (1C), 147.9(1C), 148.8 (1C) 156.2 (1C), 160.6 (1C, >C=O); MS m/z: 334.30 [M^+] calculated for $C_{16}H_{10}ClN_5O$; Elemental Analysis calculated: C, 59.36; H, 3.11; Cl, 10.95; N, 21.63; O, 4.94; Found: C, 59.27; H, 3.04; Cl, 10.87; N, 21.58; O, 4.87.

2-(4-nitrophenyl)-3-(1H-1,2,4-triazol-3-yl)quinazolin-4(3H)-one(2c)

Color: dark yellow powder; m.p. 186-188°C; % yield: 68-70%; IR (KBr, cm^{-1}): 3352.18 (Ar C-H), 1625.25 (C=O), 1567.72 (C=C), 1599.82 (C=N), 1509.23 (-NO2), 1335.11 (C-N), (N-N) ;^{1}HNMR (400 MHz, DMSO-d_6): δ 7.50 (1H, d, C-$H_{Quinazolinone}$), 7.68 (1H, s, $ArCH_{Quinazolinone}$), 7.84 (1H, d, $ArCH_{Quinazolinone}$), 8.12 (1H, s, $ArCH_{Quinazolinone}$), 7.62 (1H, d, C-$H_{triazole}$), 8.09 (2H, m, ArCH), 8.41 (2H, m, ArCH), 14.47 (1H, s, $NH_{triazole}$); ^{13}CNMR (125 MHz, DMSO-d_6), δppm: 120.8 (1C), 124.01 (2C), 126.6-126.7 (2C), 127.3 (1C), 129.7 (2C), 133.4 (1C), 134.6 (1C), 146.0 (1C), 147.9(1C), 148.7 (1C), 149.4 (1C), 156.2 (1C), 160.6 (1C, >C=O); MS m/z: 334.17 [M^+] calculated for $C_{16}H_{10}N_6O_3$; Elemental Analysis calculated: C, 57.49; H, 3.02; N, 25.14; O, 14.36; Found: C, 57.56; H, 3.09; N, 25.24; O, 14.45.

2-(p-tolyl)-3-(1H-1,2,4-triazol-3-yl)quinazolin-4(3H)-one (2d)

Color: Light yellow powder; m.p. 190-192°C; % yield: 68-70%; IR (KBr, cm^{-1}): 3043.85 (Ar C-H), 1646.95 (C=O), 1593.56 (C=C), 1486.68 (C=N), 1443.85 (C-N), 877.36 (N-N);^{1}HNMR (400 MHz, DMSO-d_6): δ 2.42 (3H, s, -CH_3), 7.28 (2H, d, ArCH), 7.50 (1H, d, C-H $_{Quinazolinone}$), 7. 64 (2H, d, ArCH), 7.68 (1H, s, ArCH $_{Quinazolinone}$), 7.84 (1H, d, ArCH $_{Quinazolinone}$), 8.13 (1H, s, ArCH $_{Quinazolinone}$), 7.62 (1H, d, C-H $_{triazole}$), 14.47 (1H, s, NH $_{triazole}$); ^{13}CNMR (125 MHz, DMSO-d_6), δppm: 21.3 (1C, -CH_3), 120.8 (1C), 125.6 (2C), 126.6-126.7 (2C), 127.3 (1C), 129.1-130.3 (4C), 133.4 (1C), 139.8 (1C), 146.0 (1C), 147.9(1C), 148.7 (1C), 156.2 (1C), 160.6 (1C, >C=O); MS m/z: 303.14 [M^+] calculated for $C_{17}H_{13}N_5O$; Elemental Analysis calculated: C, 67.32; H, 4.32; N, 23.09; O, 5.27; Found: C, 67.26; H, 4.29; N, 23.01; O, 5.15.

2-(4-fluorophenyl)-3-(1H-1,2,4-triazol-3-yl)quinazolin-4(3H)-one (2e)

Color: Reddish yellow powder; m.p. 209-211°C; % yield: 68-70%; IR (KBr, cm^{-1}): 3024.27 (Ar C-H), 1618.90 (C=O), 1572.20 (C=C), 1482.52 (C=N), 1331.64 (C-H), 1092.44 (C-N), 842.91 (N-N);^{1}HNMR (400 MHz, DMSO-d_6): δ 7.38 (2H, d, ArCH), 7.50 (1H, d, C-H $_{Quinazolinone}$), 7.68 (1H, s, ArCH $_{Quinazolinone}$), 7.84 (1H, d, ArCH $_{Quinazolinone}$), 8.13 (1H, s, ArCH $_{Quinazolinone}$), 7.62 (1H, d, C-H $_{triazole}$), 8.08 (2H, d, ArCH), 14.47 (1H, s, NH $_{triazole}$); ^{13}CNMR (125 MHz, DMSO-d_6), δppm: 115.56 (2C), 120.82 (1C), 124.26 (1C), 126.63-126.72 (2C), 127.34 (1C), 130.52 (2C), 133.46 (1C), 146.02 (1C), 147.94(1C), 148.72 (1C), 156.21 (1C), 160.63 (1C, >C=O), 164.37 (1C); MS m/z: 307.09 [M^+] calculated for $C_{16}H_{10}FN_5O$; Elemental Analysis calculated: C, 62.54; H, 3.28; F, 6.18; N, 22.79; O, 5.21; Found: C, 62.62; H, 3.36; F, 6.24; N, 22.83; O, 5.27.

2-(4-methoxyphenyl)-3-(1H-1,2,4-triazol-3-yl)quinazolin-4(3H)-one (2f)

Color: yellowish white powder; m.p. 188-200°C; % yield: 62-65%; IR (KBr, cm^{-1}): 3251.20 (Ar C-H), 16161.69 (C=O), 1527.78 (C=C), 1445.82 (C=N), 1133.85 (C-H), 830.40 (N-N);^{1}HNMR (400 MHz, DMSO-d_6): δ 3.81 (1C, OCH_3), 7.05 (2H, d, ArCH), 7.33 (2H, d, ArCH), 7.50 (1H, d, C-H $_{Quinazolinone}$), 7.68 (1H, s, ArCH $_{Quinazolinone}$), 7.84 (1H, d, ArCH $_{Quinazolinone}$), 8.13 (1H, s, ArCH $_{Quinazolinone}$), 7.62 (1H, d, C-H $_{triazole}$), 14.47 (1H, s, NH $_{triazole}$); ^{13}CNMR (125 MHz, DMSO-d_6), δppm: 58.82 (1C), 114.46 (2C), 120.82 (1C), 120.98(1C), 126.63-126.72 (2C), 127.34 (1C), 131.46 (2C), 133.65 (1C), 146.02 (1C), 147.94 (1C), 148.72 (1C), 156.21 (1C), 160.63 (1C, >C=O), 162.03 (1C); MS m/z: 319.23 [M^+] calculated for $C_{17}H_{13}N_5O_2$; Elemental Analysis calculated: C, 63.94; H, 4.10; N, 21.93; O, 10.02; Found: C, 64.02; H, 4.16; N, 22.01; O, 10.08.

2-(4-hydroxyphenyl)-3-(1H-1,2,4-triazol-3-yl)quinazolin-4(3H)-one (2g)

Color: yellowish white powder; m.p. 185-187°C; % yield: 60-62%; IR (KBr, cm^{-1}): 3248.90 (Ar C-H), 1614.85 (C=O), 1527.20 (C=C), 1445.49 (C=N), 1235.05 (C-N), 827.37 (N-N) 3248.90 (Ar C-H), 1614.85 (C=O), 1527.20 (C=C), 1445.49 (C=N), 1235.05 (C-N), 827.37 (N-N) ;^{1}HNMR (400 MHz, DMSO-d_6): δ 6.83 (2H, d, ArCH), 7.16 (2H, d, ArCH), 7.50 (1H, d, C-H $_{Quinazolinone}$), 7.68 (1H, s, ArCH $_{Quinazolinone}$), 7.84 (1H, d, ArCH $_{Quinazolinone}$), 8.13 (1H, s, ArCH $_{Quinazolinone}$), 7.62 (1H, d, C-H $_{triazole}$), 9.67 (1H, s, OH), 14.47 (1H, s, NH $_{triazole}$); ^{13}CNMR (125 MHz, DMSO-d_6), δppm: 116.01 (2C), 120.82 (1C), 121.23(1C), 126.64-126.73 (2C), 127.34 (1C), 131.86 (2C), 133.46 (1C), 146.02 (1C), 147.94 (1C), 148.73 (1C), 156.21 (1C), 159.93 (1C), 160.62 (1C, >C=O); MS m/z: 305.14 [M^+] calculated for $C_{16}H_{11}N_5O_2$; Elemental Analysis calculated: C, 62.95; H, 3.63; N, 22.94; O, 10.48; Found: C, 62.86; H, 3.57; N, 22.85; O, 10.42.

2-(4-isopropylphenyl)-3-(1H-1,2,4-triazol-3-yl)quinazolin-4(3H)-one (2h)

Color: yellowish white powder; m.p. 182-184°C; % yield: 66-68%; IR (KBr, cm^{-1}): 3249.59 (Ar C-H), 2977.97 (Al C-H), 1615.85 (C=O), 1527.97 (C=C), 1445.60 (C=N), 1235.55 (C-N), 828.41 (N-N); ^{1}HNMR (400 MHz, DMSO-d_6): δ 1.20 (6H, s, -CH_3), 5.02 (1H, >CH-), 7.36 (2H, d, ArCH), 7.50 (1H, d, C-H $_{Quinazolinone}$), 7.68 (1H, s, ArCH $_{Quinazolinone}$), 7.71 (2H, d, ArCH), 7.84 (1H, d, ArCH $_{Quinazolinone}$), 8.13 (1H, s, ArCH $_{Quinazolinone}$), 7.62 (1H, d, C-H $_{triazole}$), 14.47 (1H, s, NH $_{triazole}$); ^{13}CNMR (125 MHz, DMSO-d_6), δppm: 23.34 (2C), 33.26 (1C), 120.82 (1C), 125.87-126.21 (3C), 126.64-126.73 (2C), 127.34 (1C), 130.09 (2C), 133.46 (1C), 146.02 (1C), 147.94 (1C), 148.73 (1C), 149.83 (1C), 156.21 (1C), 160.62 (1C, >C=O); MS m/z: 330.19 [M^+] calculated for $C_{19}H_{17}N_5O$; Elemental Analysis calculated: C, 68.87; H, 5.17; N, 21.13; O, 4.83; Found: C, 68.82; H, 5.11; N, 21.08; O, 4.77.

2-(2, 4-dichlorophenyl)-3-(1H-1,2,4-triazol-3-yl)quinazolin-4(3H)-one (2i)

Color: yellowish white; m.p. 170-172°C; % yield: 63-65%; IR (KBr, cm^{-1}): 3092.17 (Ar C-H), 1622.44 (C=O), 1574.62 (C=C), 1481.69 (C=N), 1337.30 (C-N), 1187.31 (C-H), 824.74 (N-N) ;^{1}HNMR (400 MHz, DMSO-d_6): δ 7.38 (1H, d, ArCH), 7.50 (1H, d, C-H $_{Quinazolinone}$), 7.68 (1H, s, ArCH $_{Quinazolinone}$), 7.69-7.70 (2H, d, ArCH), 7.84 (1H, d, ArCH $_{Quinazolinone}$), 8.13 (1H, s, ArCH $_{Quinazolinone}$), 7.62 (1H, d, C-H $_{triazole}$), 14.47 (1H, s, NH $_{triazole}$); ^{13}CNMR (125 MHz, DMSO-d_6), δppm: 120.82 (1C), 121.13 (1C), 126.63-126.74 (2C), 127.02 (1C), 127.34-127.44 (2C), 128.94-129.12 (2C), 132.24 (1C), 133.47 (1C), 146.02 (1C), 147.93 (1C), 148.73 (1C), 156.21 (1C), 160.62 (1C, >C=O); MS m/z: 358.09 [M^+] calculated for $C_{16}H_9Cl_2N_5O$; Elemental Analysis calculated: C, 53.65; H, 2.53; Cl, 19.79; N, 19.55; O, 4.47; Found: C, 53.57; H, 2.45; Cl, 19.66; N, 19.47; O, 4.39.

2-(2,4-dinitrophenyl)-3-(1H-1,2,4-triazol-3-yl)quinazolin-4(3H)-one (2j)

Color: Dark yellow powder; m.p. 225-227°C; % yield: 68-70%; IR (KBr, cm^{-1}): 3093.80 (Ar C-H), 1616.48 (C=O), 1558.55 (C=C), 1485.85 (C=N), 1363.82 (C-N), 831.30 (N-N);^{1}HNMR (400 MHz, DMSO-d_6): δ 7.50 (1H, d, C-H $_{Quinazolinone}$), 7.68 (1H, s, ArCH $_{Quinazolinone}$), 7.84 (1H, d, ArCH $_{Quinazolinone}$), 8.13 (1H, s, ArCH $_{Quinazolinone}$), 8.32 (1H, s, ArCH), 8.74 (1H, s, ArCH), 9.15 (1H, s, ArCH), 7.62 (1H, d, C-H $_{triazole}$), 14.47 (1H, s, NH $_{triazole}$); ^{13}CNMR (125 MHz, DMSO-d_6), δppm: 120.12-120.82 (2C), 126.53 (1C), 126.63-126.74 (2C), 127.34 (1C), 127.94 (1C), 130.14 (1C), 133.46 (1C), 145.61 (1C), 146.02 (1C), 147.93 (1C), 148.73 (1C), 150.21 (1C), 156.21 (1C), 160.62 (1C, >C=O); MS m/z: 379.29 [M^+] calculated for $C_{16}H_9N_7O_5$; Elemental Analysis calculated: C, 50.67; H, 2.39; N, 25.85; O, 21.09; Found: C, 50.74; H, 2.47; N, 25.94; O, 21.16.

2.2. Biological Evolution

2.2.1 Glycolytic enzyme inhibition study

The enzyme solution was prepared by dissolving 1 mg of the enzyme α-glycosidase (Saccharomyces cerevisiae) in 20 ml of phosphate buffer (pH 7.0) containing 40 mg bovine serum albumin (BSA). Further, it was diluted to 1:10 with a phosphate buffer solution just before use. The synthesized compounds **(2a-j)** were dissolved in 10 mM DMSO at five concentrations (25, 50, 75, 100, 125, and 150 µM), while sample

blanks were prepared using 5 µL DMSO, 250 µL p-nitrophenyl-D-glucopyranoside, and 495 µL phosphate buffer (pH 7.0). It was pre-incubated at 37°C for 5 min, and 250 µL of enzyme solution was added to initiate the reaction, which was then incubated at 37°C for precisely 15 minutes. A UV-visible Spectrophotometer was utilized to measure the amount of p-nitrophenol produced by measuring the absorbance of compounds against the sample blank containing DMSO at 400 nm when the reaction was stopped through the addition of 1000 µL of a 200 mM sodium carbonate (Na_2CO_3) solution [11].

In Vitro Antiglycation Potential

Glycation of Bovine Serum Albumin

The antiglycation activity of synthesized compounds **(2a-j)** was determined using glycated BSA samples prepared by incubating BSA (10 mg/mL) with fructose (250 mM) in 200 mM phosphate buffer (pH 7.4, containing 0.02% sodium azide) along with Rutin varying concentrations of the test compounds (25, 50, 75, 100, 125, and 150 µM) at 37°C in the dark for 72 hours in sealed tubes. A positive control (BSA + fructose) was maintained under similar conditions, and all incubations were performed in triplicate. After incubation, unbound fructose was removed by dialysis against phosphate buffer (200 mM, pH 7.4) at 4°C. The resultant glycated BSA samples were analyzed for antiglycation activity by estimating fructosamine levels using the NBT assay [12, 13].

Estimation of Fructosamine

The estimation of fructosamine in glycated BSA samples was performed using the Nitro blue Tetrazolium (NBT) assay. The positive control (10 µL) and glycated sample aliquots were combined with 0.2 mL of NBT solution (0.5 mM) (NBT was prepared in 100 mM sodium carbonate buffer of pH 10.35). The resultant solutions were incubated for 30 minutes at 37°C. After incubation, the absorbance was measured at 520 nm using a UV-spectrophotometer. The percentage inhibition of fructosamine formation was calculated using the formula Inhibitory activity (%) = [(A_0 – A_1) / A_0] x 100. Where A_0 is the absorbance of the positive control (BSA + fructose) and A_1 is the absorbance of the glycated albumin samples. The assay was performed in triplicate for each compound. The lower the absorbance of the glycated albumin samples compared to the positive control, the higher the inhibitory activity against fructosamine formation. This assay provides a quantitative measure of the ability of compounds to inhibit glycation, a process crucial in preventing diabetic complications.

2.2.3 Antioxidant activity

The antioxidant potential of compounds **(2a-j)** was evaluated based on their ability to scavenge free radicals. The antioxidant potential of the synthesized compounds was assessed via the DPPH assay, which evaluates their ability to scavenge free radicals. A 10 mM stock solution was prepared in ethanol, and a series of dilutions (25, 50, 75, 100, 125, and 150 µM) of the synthesized compounds were prepared in appropriate solvents. For the assay, 1 ml of each diluted sample was mixed with 3 ml of a freshly prepared solution of 0.1 mM 2, 2-diphenyl-1-picrylhydrazyl (DPPH) and incubated for 30 minutes in the dark at room temperature. For the absorbance at 517 nm, a UV-Vis spectrophotometer was used to measure a control solution containing only DPPH and DMSO. To calculate the percentage of scavenging activity using the formula: Inhibitory activity (%) = [(A_c – A_s) / A_c] x 100. Where A_c and A_s represent the absorbance of the control and the sample solution, respectively. The assay was performed in triplicate for each compound. The antioxidant activity was compared to the standard antioxidant, ascorbic acid, and the inhibitory concentration (IC_{50}) for 50% inhibition was determined for the synthesized compounds [13].

2.2.4 Molecular docking study

Molecular docking is a computational tool used in drug discovery to predict ligand-protein interactions and binding affinities, aiding in the optimization of molecular structures and identification of potential ligands [14]. The interaction of the synthesized quinazoline derivatives (2a-l) and the standard compound Rutin, with human serum albumin-fructose complex (PDB ID: 4IW1) was evaluated using molecular docking [15]. The target protein structure was downloaded from the Protein Data Bank (http://www.rcsb.org/pdb).ChemDraw version 22.2.0 (64-bit) was used to develop the two-dimensional (2D) chemical structures of the synthesized quinazoline derivatives (2a–j) and Rutin. These 2D structures were imported into Chem3D version 22.2.0 (64-bit) to 3D molecular structures [16]. The MM2 force field algorithm was used to structurally optimize the 3D geometries to achieve energetically minimized conformations. The optimized structures were then exported and saved in .pdb format for further molecular docking analysis. The molecular docking simulations were performed by using Molegro Virtual Docker v.6.0. The estimated surface area and volume of the active site were depicted in Figure 1. A spherical search space with a radius of 15.0 A centered at the binding site (X: 2.70, Y: -0.38, Z: 15.63) was

set using a grid spacing of 0.30 A, a population size of 50 and 1500 iterations, and ten runs per ligand. [17, 18].

3. RESULT AND DISCUSSION

3.1 Chemistry

A two-step synthetic strategy (Scheme 1) was established to access quinazolinone-triazole hybrids (2a-j), which involved anthranilic acid as starting material. The reaction began when the substituted benzoyl chlorides were reacted with Anthranillic acid in dry pyridine at a controlled temperature to produce the benzoxazinone derivatives (1a-j). The reaction went well, which was indicated by the crystalline products obtained after neutralization and crystallization. On Sep 2, these benzoxazinone intermediates were further allowed to react with 4-amino-1,2,4-triazole by reflux in dry pyridine, which led to the opening of the ring and the subsequent cyclization to produce the Quinazolinone-triazole hybrids 2a-f. The yield of compound 2a was moderate (66-68%), and it was obtained in the form of canary yellow powder with high purity, indicated by a sharp melting point of 186-188℃.

The structure of these synthesized hybrids was confirmed through spectral analysis such as IR, NMR, and Mass spectroscopy. The characteristic absorption was detected on the IR spectrum for aromatic C-H, carbonyl group, C=N, and N-N functionalities at 3064 cm^{-1}, 1667 cm^{-1}, 1526 cm^{-1}, and 838 $cm^{-1,}$ respectively. Subsequently, the ^{1}HNMR spectrum displayed multiplets between δ 7.49-812 ppm and a singlet at 14.46 ppm, which is attributed to the aromatic protons and proton of NH of triazole ring, respectively. This was further supported by the ^{13}C NMR, which showed signals in the predicted regions of aromatic and heterocyclic carbons, specifically a very characteristic signal at δ 160.5 ppm in the Quinazolinone carbonyl carbon. The mass spectrum showed that the molecular ion peak at m/z 289 was in line with the calculated molecular weight of $C_{16}H_{11}N_5O$. The elemental analysis also closely aligns with calculated values, confirming the composition of the synthesized compound. In general, the synthetic procedure was effective and consistent in the synthesis of Quinazolinone-triazole hybrids that undergo further pharmacological investigation.

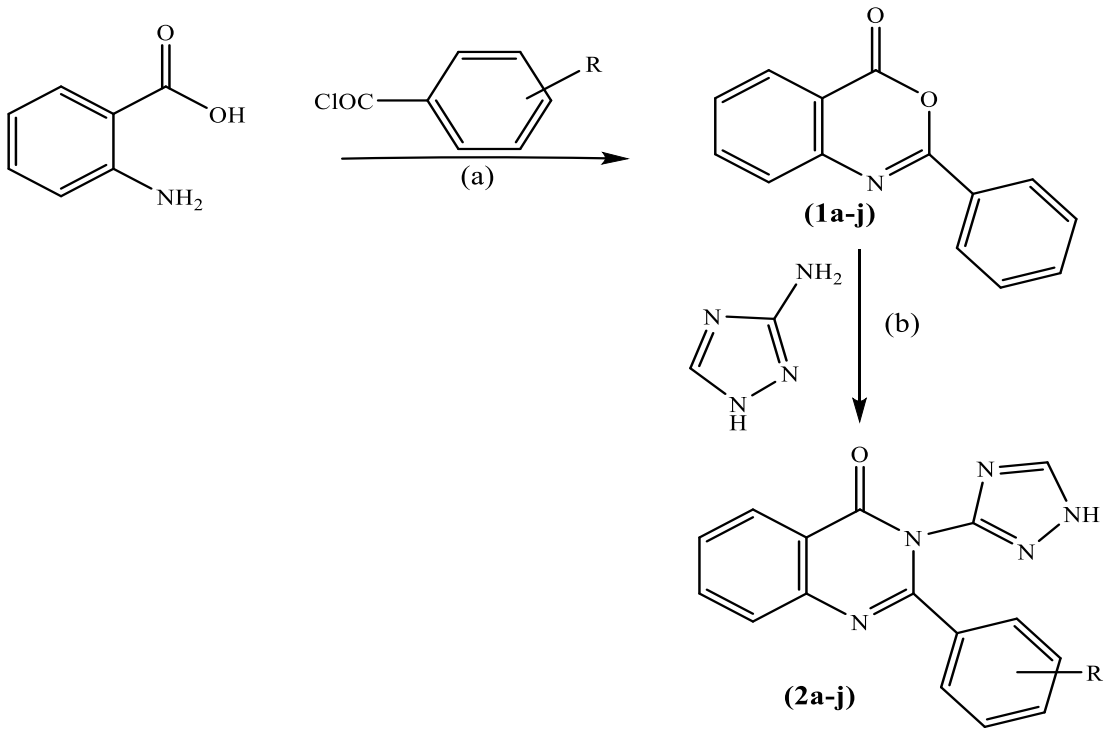

Where, R; 2a=H, 2b=4-Cl, 2c=4-NO_2, 2d=4-CH_3, 2e= 4-f, 2f=4-OCH_3, 2g= 4-OH, 2h=4-$CH(CH_3)_2$, 2i= 2-Cl, 4-Cl, 2j=2-NO_2, 4-NO_2,

Scheme 1: Schematic representation of the synthesis of Quinazolinone-triazole Hybrids (2a-j)

Reagents and Reaction Conditions: (a) Benzoyl chloride, Pyridine, Stirring at Room temperature, (b) 4-amino triazole, dry pyridine, Reflux for 5 hours at 90-100℃.

3.2 Biological Activities

3.2.1 Glycolytic enzyme inhibition study

A methodological screening of the inhibitory activity on α-glycosidase of the novel Quinazolinone-triazole hybrids was carried out by determining their half maximal dose of inhibitory activity (IC_{50}) values in μM.

The data obtained showed that the strongest inhibitory activity against α-glycosidase, with IC_{50} values of 58.33±0.88 µM, 62.66±0.88 µM, and 46.00±1.15 µM corresponding to compounds 2d, 2g, and 2h. Outperforming standard α-glycosidase inhibitor rutin (IC_{50} value 75.33±1.45 µM). On the other hand, the low to moderate activity was recorded with other synthesized compounds that portrayed relatively low IC_{50} values, indicating mild to moderate inhibitory activity against α-glycosidase. Collectively, the above findings suggest that the compounds bearing electron-donating groups enhance the α-glycosidase inhibitory activity compared to compounds with other substituents (See figure 1).

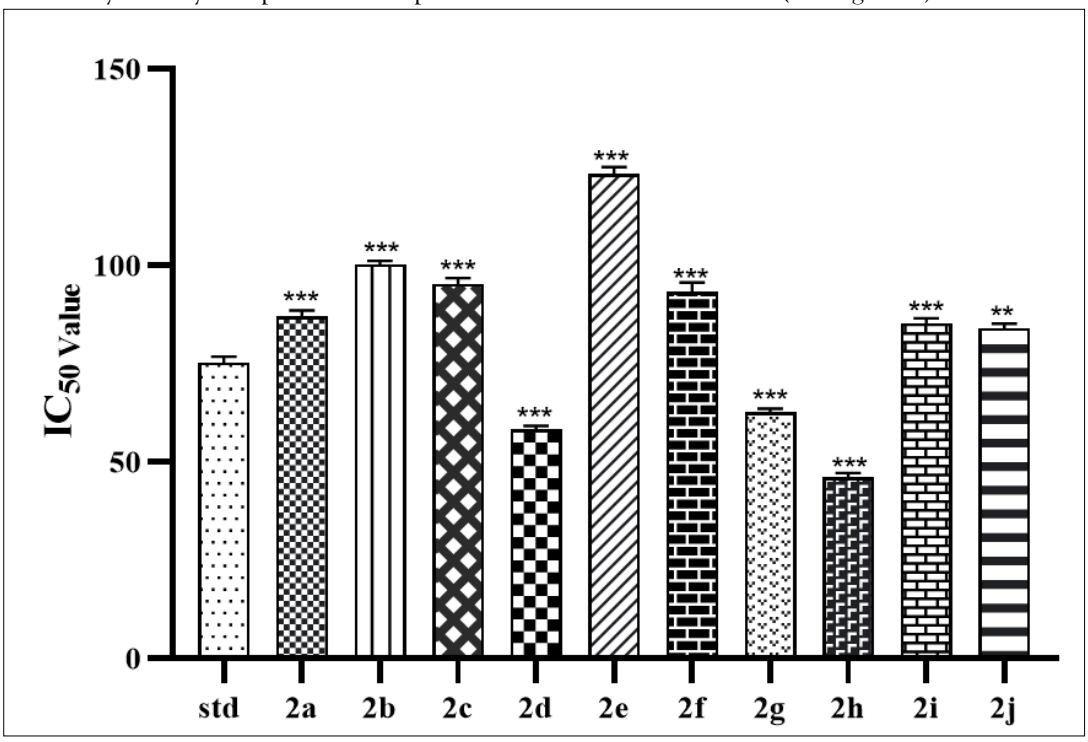

Figure_1. Glycolytic enzyme inhibition potential of synthesized Quinazolinone-triazole hybrids (2a-j) and standard drug (Rutin). Data are expressed as mean ± SEM (n = 3). Dunnett's post hoc test was employed with a one-way ANOVA in the statistical analysis. At *p < 0.05, **p < 0.01, and ***p < 0.001, significance was considered.

Table 1. α-glycosidase inhibitory Potential of Quinazolinone-triazole hybrids (2a-j)

Compound ID	**Glycolytic activity (IC_{50} value)**
Rutin	75.33±1.45
2a	87.00±1.52
2b	100.33±0.88
2c	95.33±1.45
2d	58.33±0.88
2e	123.33±1.76
2f	93.33±2.33
2g	62.66±0.88
2h	46.00±1.15
2i	85.33±1.20
2j	84.00±1.15

3.2.2 In vitro Antiglycation Potential

The in vitro Anti-glycation activity of synthesized compounds (2a-2l) was evaluated by employing a Glucose-Bovine serum albumin (BSA) assay. BSA incubated with fructose served as a positive control under identical conditions. Antiglycation efficacy was quantified by measuring fructosamine levels, a stable early-stage glycation product formed via non-enzymatic reaction between reducing sugars and protein amino groups. As a key biomarker, fructosamine provides a reliable indicator of protein glycation and the inhibitory potential of the test compounds. The extent of glycation inhibition was measured by determining the IC_{50} values, which denote the concentration of the test compound required to achieve 50% inhibition of fructosamine formation, as presented in Table 3. Notably, among the synthesized

compounds, **2d**, **2g**, and **2h** exhibited the most prominent Antiglycation activity, with the lowest IC_{50} values of 66.66±0.88µM, 75.00±1.52µM, and 53.33±1.76 µM, respectively (Figure 2). These results suggest a higher affinity of these compounds for glycation intermediates as compared to rutin, a recognized positive control that also displayed significant inhibitory activity with an IC_{50} value of 96.00±1.15 µM. The result indicates that the presence of electron-donating groups on the aromatic ring enhances the electron density, consequently increasing the nucleophilicity and reactivity of these compounds towards reactive carbonyl species (RCS) and glycation intermediates. This electronic influence effectively impedes the formation of both Schiff bases and their subsequent isomerization to Amadori products, thus leading to a significant interruption of the early-stage glycation pathway.

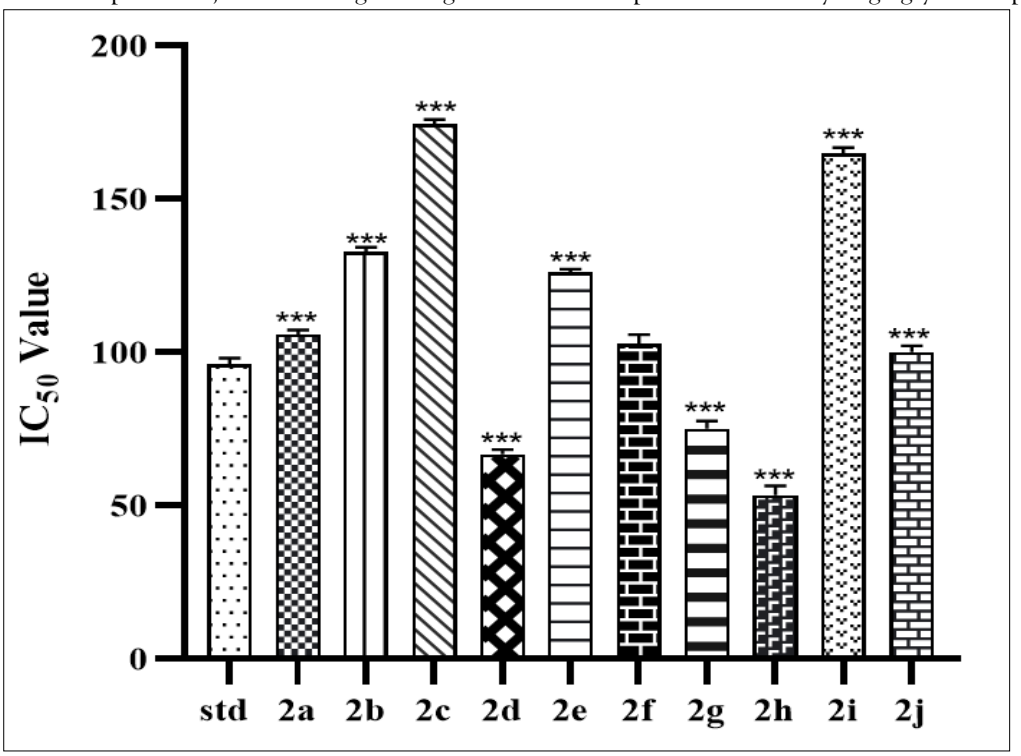

Figure_2. Antiglycation potential of Quinazolinone-triazole hybrids (2a-j) assessed by estimation of fructosamine. All values are presented in mean ± SEM (n=3). Statistical analysis was performed using one-way ANOVA followed by Dunnett's post hoc test, significance levels: *p < 0.05, **p < 0.01, *** p < 0.001.

Table 2. In-vitro Antiglycation Potential of Quinazolinone-triazole hybrids (2a-j) assessed through fructosamine level estimation

Compound ID	**IC_{50} Values**
Rutin	96.00±1.15
2a	105.66±0.88
2b	132.66±0.88
2c	174.33±0.88
2d	66.66±0.88
2e	126.00±0.57
2f	102.66±1.52
2g	75.00±1.52
2h	53.33±1.76
2i	164.66±1.20
2j	100.00±1.15

3.2.3 Antioxidant Activity

The novel compounds (2a-j) were evaluated to determine their antioxidant capacity by the addition of DPPH radical scavenging. These compounds lead to the reduction of the absorbance at wavelength 517 nm by reacting with DPPH and electron donation or acceptance, thus implying their functionality against the free radicals. The ascorbic acid served as a standard antioxidant. The IC_{50} values, which indicate the

concentration at which 50% of DPPH radicals are scavenged, were determined for each synthesized compound to assess their antioxidant potential. Among these, compounds 2d, 2g, and 2h exhibited the most potent antioxidant activity, with IC_{50}values of 25.66±0.88 µM, 41.66±2.72, and 34.00±1.00 µM, respectively. The IC_{50} values indicated that both compounds were more effective antioxidants than ascorbic acid (IC_{50} 37.00 ± 0.57 µM) represented in Figure 3. These results suggest that the compounds bearing electron-donating groups, like alkyl and hydroxyl, exhibited superior free radical neutralization compared to those with electron-withdrawing groups. This enhanced activity can be attributed to the electron-donating nature of these substituents, which increases the ability of the compound to donate hydrogen atoms or electrons, thus stabilizing the DPPH radical.

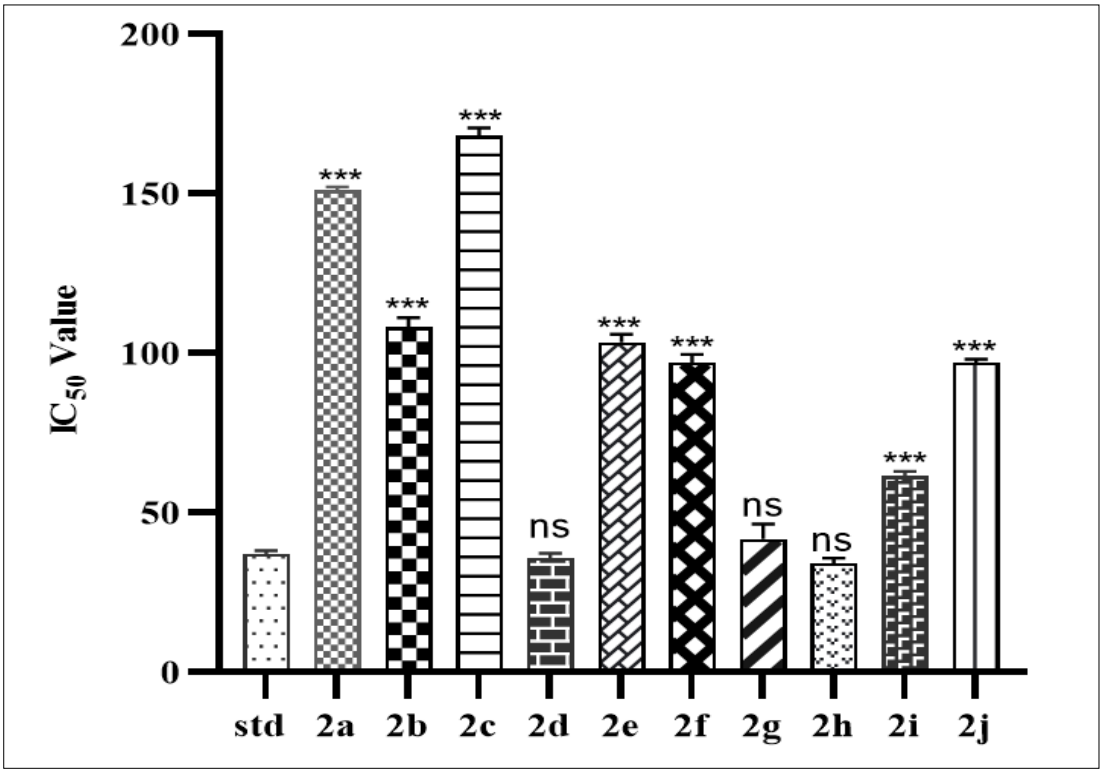

Figure_3. Antioxidant potential of synthesized Quinazolinone-triazole hybrids **(2a–j)** assessed by DPPH radical scavenging assay. All values are represented in mean ± SEM (n=3). Dunnett's post hoc test was employed following a one-way ANOVA for statistical analysis, with significance levels of *p < 0.05, **p < 0.01, and *** p < 0.001

Table 3. Antioxidant Potential of Quinazolinone-triazole Hybrids (2a-j)

Compound ID	**IC_{50} Values**
Rutin	37.00±0.57
2a	151.00±0.57
2b	108.00±1.73
2c	168.00±1.52
2d	35.66±0.88
2e	103.33±1.45
2f	97.00±1.52
2g	41.66±2.72
2h	34.00±1.00
2i	61.33±0.88
2j	97.00±0.57

3.2.4 Molecular Docking Study

Molecular docking simulations were performed for the synthesized Quinazolinone-triazole hybrids **(2a-j)** and reference drug rutin against the active site of HSA-fructose complex (PDB ID:4IW1) using Molegro Virtual Docker version 6.0 software. The docking simulations, assessed through the MolDock scoring function, demonstrated that all the synthesized compounds exhibited strong binding affinities within the

active sites of the enzymes. The MolDock scores ranged from -103.401 kcal/mol to -155.687 kcal/mol, indicating favorable interactions between the ligands and target proteins. Among the tested derivatives, compound **2g** demonstrated the lowest MolDock score, indicating the strongest binding affinity toward both target enzymes. However, the reference drug rutin revealed a lower MolDock score of -143.761kcal/mol, suggesting a relatively less stable ligand-receptor interaction. A comprehensive summary of the binding affinity, H-bond, and S-bond interaction of all the designed ligands is presented in Table 4. The docking results revealed that the enhanced binding affinities of these compounds are predominantly driven by the establishment of non-covalent interactions, including hydrogen bonding, π–π stacking, and sulfur molecule contacts with critical amino acid residues within the active site. This can be attributed to its optimal orientation and interaction geometry within the binding pocket, enabling stronger stabilization of the ligand protein complex. Among the various interactions observed, the Lys195, Ala381, Arg218, and Cys448 residues in the target protein emerged as critical binding determinants. These residues consistently formed hydrogen bonds with all synthesized compounds, as well as with rutin. Additionally, designed derivatives also exhibited prominent steric interactions with other key residues such as Lys195, Lys199, Leu198, Arg222, Trp214, and Val343, as shown in Figure 4. The protein-ligand complex interaction illustrates the binding pocket interactions of compound **2g** and the reference drug with target proteins, as shown in Figure 5. These docking results suggest that the synthesized Quinazolinone-triazole derivatives, particularly compound 2g, may serve as promising Antiglycation agents by effectively interacting with the HSA–fructose complex and potentially inhibiting advanced glycation end-product (AGE) formation through stable protein binding.

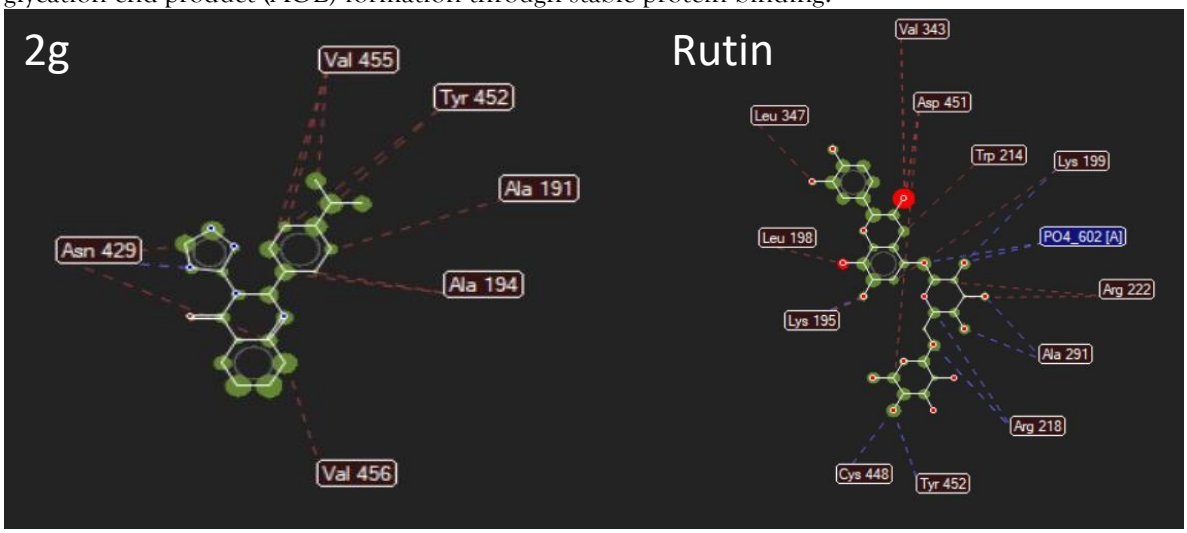

Figure 4. The protein-ligand complex interaction of compound **2g** and Rutin. The blue dotted line represents the H-bond, while the red dotted line represents the S-bond interaction with the target protein.

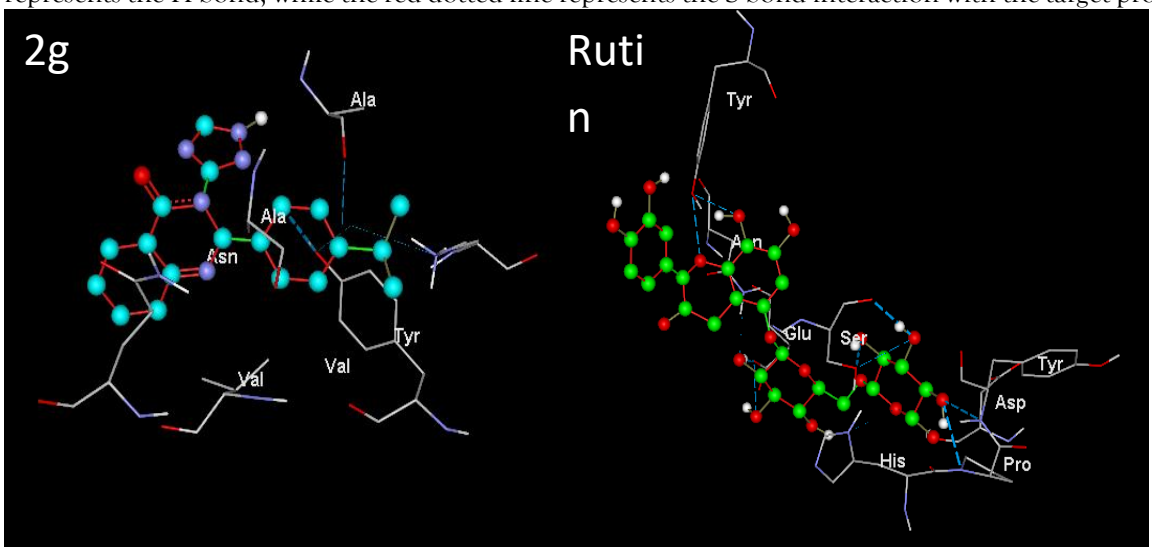

Figure 5. Binding interactions of compound 2g and rutin within the active site of the HSA–fructose complex.

Table 4: Molecular docking simulations of the synthesized compound with target proteins.

Compound ID	R	MolDock score (kcal/mol)	HBond	H-bond Interaction	S-bond interaction
Rutin	-	143.761	-1.51622	Lys195, Ala291, Lys199, Ala381, Arg218, Cys448	Lys195, Lys199, Leu198, Arg222, Trp214, Leu347, Val343, Asp451
2a	H	-117.713	-1.11077	Ala291, Ala381, Arg218, Cys448	Lys195, Arg222, Asp451
2b	4-Cl	-132.201	-0.51704	Lys195, Ala291, Arg218, Cys448	Lys195, Lys199, Leu198, Arg222, Asp451
2c	4-NO_2	-103.401	-5.97205	Lys195, Ala381, Arg218, Cys448	Ala194, Tyr452, Val456, Gln459,
2d	4-CH_3	-147.833	-1.75144	Lys195, Ala291, Lys199, Arg218,	Lys195, Arg222, Trp214, Val343, Asp451
2e	4-F	-139.621	-1.76567	Lys195, Arg218, Cys448	Lys195, Lys199, Arg222, Trp214, Val343, Asp451
2f	4-OCH_3	-152.066	-1.24058	Lys195, Lys199, Ala381, Cys448	Lys195, Lys199, Leu198, Arg222, Val343, Asp451
2g	4-OH	-155.687	-0.02134	Ala191, Lys456, Tyr452	Ala194, Tyr452, Val456, Gln459
2h	4-$CH(CH_3)_2$	-154.112	-1.14028	Lys195, Ala381, Arg218, Cys448	Lys195, Lys199, Leu198, Arg222, Trp214
2i	2-Cl, 4-Cl	-141.837	-0.05451	Lys195, Arg218, Cys448	Lys195, Lys199, Leu198, Arg222, Trp214, Val343
2j	2-NO_2, 4-NO_2	-132.485	-1.75289	Ala381, Arg218,	Ala194, Val456, Gln459

CONCLUSION

In the present study, a series of synthesized Quinazolinone-triazole hybrids (2a-j) were assessed to reflect their possible ability to counter oxidative stress, enzymatic gastrointestinal carbohydrate digestion, and protein glycation, these three major processes involved in the pathogenesis of diabetes and its complications. The synthesized compounds were found to have good pharmacological potential with significant ὰ-glucosidase, Anti-glycation, and antioxidant potential. The derivatives **2d**, **2g**, and **2h** exhibited the highest ὰ-glucosidase inhibition compared to the standard drug rutin and other derivatives. They probably do so by slowing down carbohydrate hydrolysis and glucose absorption, and provide effective action on postprandial blood glucose. They also showed Anti-glycation properties, as observed by a significant decrease in fructosamine levels, which implies their promise against preventing glycation-induced protein damage, the source of most diabetic complications. Furthermore, the antioxidant test also showed that many of the compounds, especially **2d**, **2g**, and **2h**, were effective in free radical scavenging, thus converting the oxidative stress, which is another factor that contributes to diabetes development. After thorough analysis, it is indicated that the electron-donating groups like alkyl and polar hydroxyl substituted compounds may contribute to enhancing enzyme binding affinity and increased

radical scavenging efficiency, thus raising the overall pharmacological value of the compounds. In conclusion, the multifunctional properties of these synthesized compounds, especially those bearing alkyl and hydroxyl groups, make them promising lead candidates for further development in the treatment or prevention of diabetes and its oxidative complications.

REFERENCES

1.A. Bhattacherjee, K. Dhara, AS. Chakraborti, ''Bimolecular interaction of argpyrimidine (a Maillard reaction product) in in vitro non-enzymatic protein glycation model and its potential role as an antiglycating agent'', International Journal of Biological Macromolecules, vol. 102, pp. 1274-85, 2017.
2.F. Liu, N. Delchier, Y. Bao, C. Xie, Y. Li, X. Liu, X. Yu, L. Li, M. Jin, JK. Yan, ''Chemical Oxidation of B Vitamins in Food Systems: Mechanisms, Matrix Effects, and Preservation Strategies'', Comprehensive Reviews in Food Science and Food Safety, vol. 24, pp. 70-78, 2025.
3.J. Peng, G. Liang, W. Wen, W. Huang, Y. Qiu, G. Xiao, Q. Wang, ''Blueberry anthocyanins extract inhibits advanced glycation end-products (AGEs) production and AGEs-stimulated inflammation in RAW264. 7 cells'', Journal of the Science of Food and Agriculture, vol. 104, pp. 75-82, 2024.
4.B. Wang, T. Jiang, Y. Qi, S. Luo, Y. Xia, B. Lang, B. S. Zhang, ''AGE-RAGE axis and cardiovascular diseases: pathophysiologic mechanisms and prospects for clinical applications'', Cardiovascular Drugs and Therapy, vol. 5, pp. 1-8, 2024.
5.S.A. Kavitha, S. Zainab, Y.S. Muthyalaiah, C.M. S. John, Arockiasamy, ''Mechanism and implications of advanced glycation end products (AGE) and its receptor RAGE axis as crucial mediators linking inflammation and obesity'', Molecular Biology Reports, vol. 52, pp. 556-562, 2025.
6.W.N. Hauwanga, T.Y. Abdalhamed, L.A. Ezike, I.S.Chukwulebe, A.K. Oo, A. Wilfred, A.R. Khan, J. Chukwuwike, E. Florial, H. Lawan, A. Felix, ''The pathophysiology and vascular complications of diabetes in chronic kidney disease: A comprehensive review'',.
7.A. Sharma, R. Dubey, R. Bhupal, P. Patel, S.K.Verma, S. V. Kaya, ''Asati An insight on medicinal attributes of 1, 2, 3-and 1, 2, 4-triazole derivatives as alpha-amylase and alpha-glucosidase inhibitors'', Molecular Diversity, vol. 23, pp. 1-30, 2023.
8.A. Haque, M.W. Khan, K.M. Alenezi, R. Soury, M.S. Khan, S. Ahamad, M. Mushtaque, D. Gupta, ''Synthesis, Characterization, Antiglycation Evaluation, Molecular Docking, and ADMET Studies of 4-Thiazolidinone Derivatives. ACS omega'', , vol. 28, pp. 1810-20, 2023.
9.F.A.Qais, T. Sarwar, I. Ahmad, R.A. Khan, S.A. Shahzad, F.M. Husain, ''Glyburide inhibits non-enzymatic glycation of HSA: An approach for the management of AGEs associated diabetic complications'', International Journal of Biological Macromolecules, vol. 169, pp. 143-152, 2021.
10. R. Thilagavathy, H.P. Kavitha, R. Arulmozhi, J.P. V. Vennila, ''Manivannan 2-Phenyl-4H-3, 1-benzoxazin-4-one'', Structure Reports, vol. 65, pp. 127-135, 2009.
11. S. Dubey, A. Ganeshpurkar, A. Ganeshpurkar, D. N. Bansal, Dubey, ''Glycolytic enzyme inhibitory and antiglycation potential of rutin'', Future Journal of Pharmaceutical Sciences, vol. 3, pp. 158-162, 2017.
12. Sadowska-Bartosz, S. Galiniak, G. Bartosz, ''Kinetics of glycoxidation of bovine serum albumin by glucose, fructose and ribose and its prevention by food components'', Molecules, , vol. 19, pp. 1828-49, 2014.
13. P. Malik, T.K. Mukherjee, ''Immunological methods for the determination of AGE-RAGE axis generated glutathionylated and carbonylated proteins as oxidative stress markers'', Methods, , vol. 203, pp. 354-63, 2022.
14. G.M. M. Morris, Lim-Wilby, ''Molecular docking. In Molecular modeling of proteins'', Totowa, NJ: Humana Press, vol. 2, pp. 365-382, 2008.
15. M. Shaikh, S. Siddiqui, H. Zafar, U. Naqeeb, F. Subzwari, R. K.M. Imad, M.I. Choudhary, ''Antiglycation activity of triazole Schiff's bases against fructose-mediated glycation: in vitro and silico study'', Medicinal Chemistry, vol. 16, pp. 575-591, 2020.
16. G.M. Morris, M. Lim-Wilby, ''Molecular docking- In Molecular modeling of proteins 2008 Jul (pp. 365-382). Totowa, NJ: Humana Press.Z. Li, H. Wan, Y. Shi, P. Ouyang, Personal experience with four kinds of chemical structure drawing software: review on ChemDraw, ChemWindow, ISIS/Draw, and ChemSketch, J. Chem. Inf. Comput. Sci
17. A.R. Puspaningtyas, ''Docking studies of Physalis peruviana ethanol extract using the molegro virtual docker on insulin tyrosine kinase receptor as an antidiabetic agent'', International Current Pharmaceutical Journal, vol. 8, pp. 265-259, 2014.
18. S. Kusumaningrum, E. Budianto, S. Kosela, W. Sumaryono, F. Juniarti, ''The molecular docking of 1, 4-naphthoquinone derivatives as inhibitors of Polo-like kinase 1 using Molegro Virtual Docker'', Journal of Applied Pharmaceutical Science, vol. 27, pp. 47-53, 2014. 2014 Nov 27;4(11):047-53.